THE JOURNAL OF BIOLOGICAL CHEMISTRY VOL. 283, NO. 25, pp. 17662–17671, June 20, 2008

Store-dependent and -independent Modes Regulating Ca^{2+} Release-activated Ca^{2+} Channel Activity of Human Orai1 and Orai3*

Received for publication, February 26, 2008, and in revised form, April 16, 2008 Published, JBC Papers in Press, April 17, 2008, DOI 10.1074/jbc.M801536200

Shenyuan L. Zhang[1], J. Ashot Kozak[1,2], Weihua Jiang, Andriy V. Yeromin, Jing Chen, Ying Yu, Aubin Penna, Wei Shen, Victor Chi, and Michael D. Cahalan[3]

From the Department of Physiology and Biophysics, University of California, Irvine, California 92697

We evaluated currents induced by expression of human homologs of Orai together with STIM1 in human embryonic kidney cells. When co-expressed with STIM1, Orai1 induced a large inwardly rectifying Ca^{2+}-selective current with Ca^{2+}-induced slow inactivation. A point mutation of Orai1 (E106D) altered the ion selectivity of the induced Ca^{2+} release-activated Ca^{2+} (CRAC)-like current while retaining an inwardly rectifying *I-V* characteristic. Expression of the C-terminal portion of STIM1 with Orai1 was sufficient to generate CRAC current without store depletion. 2-APB activated a large relatively non-selective current in STIM1 and Orai3 co-expressing cells. 2-APB also induced Ca^{2+} influx in Orai3-expressing cells without store depletion or co-expression of STIM1. The Orai3 current induced by 2-APB exhibited outward rectification and an inward component representing a mixed calcium and monovalent current. A pore mutant of Orai3 inhibited store-operated Ca^{2+} entry and did not carry significant current in response to either store depletion or addition of 2-APB. Analysis of a series of Orai1–3 chimeras revealed the structural determinant responsible for 2-APB-induced current within the sequence from the second to third transmembrane segment of Orai3. The Orai3 current induced by 2-APB may reflect a store-independent mode of CRAC channel activation that opens a relatively nonselective cation pore.

Store-operated Ca^{2+} entry (SOCE)[4] is essential for Ca^{2+} homeostasis in many cell types (1) and is of particular importance for the immune response by enabling Ca^{2+} influx in T cells that triggers changes in gene expression following T cell receptor engagement (2–5). In T cells and other hematopoietic cells, Ca^{2+} entry following store depletion is mediated by low conductance, Ca^{2+}-selective, inwardly rectifying Ca^{2+} release-activated Ca^{2+} (CRAC) channels (6–9). Two proteins that are required for CRAC channel activity have been identified recently by RNAi screening (10–14). STIM1 initiates the process of store-operated Ca^{2+} influx by sensing the depletion of Ca^{2+} from the lumen of the endoplasmic reticulum store (11, 12, 15). It then migrates to the plasma membrane and forms aggregates at plasma membrane sites of Ca^{2+} entry and interacts either directly or in a complex with Orai1 (11, 12, 15–19). Orai in *Drosophila* and Orai1 in human cells have been shown to embody the CRAC channel, by the criterion that ion selectivity is dramatically altered upon mutation of a conserved glutamate to aspartate in the loop between the first two putative transmembrane segments (18, 20–22).

The small amplitude of native CRAC current in lymphocytes and other cells has hampered efforts to characterize the channel biophysical properties. Recent overexpression studies have shown that STIM1 and Orai1 are required for functional CRAC current and that their co-expression leads to greatly amplified CRAC currents (14, 23–25). The ability to record large CRAC currents in a heterologous system, such as transfected HEK293 cells, provides an opportunity to examine channel properties in greater detail and to understand previously described CRAC-related phenomena at the molecular level.

2-Aminoethyl diphenylborinate (2-APB) is a membrane-permeable modulator of many ion channels, including $Ins(1,4,5)P_3$ receptors (26) and TRPV1, TRPV2, and TRPV3 channels (27–30). In native and overexpression systems, it can potentiate SOCE or CRAC current at low concentrations (<5 μM) and inhibit both at higher concentrations (14, 15, 31–33).

Here we compare properties of CRAC current and Ca^{2+} influx induced by expression of the three human Orai family members (wild-type and mutants) separately or together in combination with STIM1 or a C-terminal portion of STIM1 to evaluate the molecular requirements for functional CRAC channels in HEK cells.

* This work was supported, in whole or in part, by a National Institutes of Health grant (to M. D. C.). This work was also supported by a University of California, Irvine, faculty career development award (to J. A. K.) and by fellowships from The George E. Hewitt Foundation (to S. L. Z.) and the American Heart Association (to Y. Y.). The costs of publication of this article were defrayed in part by the payment of page charges. This article must therefore be hereby marked "*advertisement*" in accordance with 18 U.S.C. Section 1734 solely to indicate this fact.

[S] The on-line version of this article (available at http://www.jbc.org) contains supplemental Figs. S1–S8.

[1] Both authors contributed equally to this work.

[2] Present address: Dept. of Neuroscience, Cell Biology, and Physiology, Wright State University, Biological Sciences Bldg., Rm. 122, Dayton, OH 45435.

[3] To whom correspondence should be addressed: 285 Irvine Hall, Dept. of Physiology and Biophysics, University of California, Irvine, CA 92697. Tel.: 949-824-7776; Fax: 949-824-3143; E-mail: mcahalan@uci.edu.

[4] The abbreviations used are: SOCE, Store-operated Ca^{2+} entry; HEK, human embryonic kidney; CRAC, Ca^{2+} release-activated Ca^{2+}; 2-APB, 2-aminoethyl diphenylborinate; GFP, green fluorescent protein; RNAi, RNA interference; siRNA, short interfering RNA; RT, reverse transcription; HA, hemagglutinin; PBS, phosphate-buffered saline; HEDTA, *N*-(2-hydroxyethyl)ethylenediaminetriacetic acid; TG, thapsigargin; h, human; MIC, Mg^{2+}-inhibited cation; WT, wild type; TM, transmembrane; ER, endoplasmic reticulum.

EXPERIMENTAL PROCEDURES

Cell Culture and Transfection—Human embryonic kidney (HEK) 293 cells or Jurkat E6–1 T cells (ATCC) were maintained and propagated as recommended by the ATCC. Jurkat cells were transfected using a Nucleofector (Amaxa) following the manufacturer's protocol. HEK293 cells were transfected using Polyfect (Qiagen) or Lipofectamine 2000 (Invitrogen) reagents and used after 12 h for $[Ca^{2+}]_i$ imaging, patch clamp electrophysiology, RT-PCR analysis, or Western blotting and after 48 h for co-immunoprecipitation.

Molecular Cloning and Mutagenesis—The generation of pcDNA3/hSTIM1 was described previously (12). Full-length hOrai2 cDNA was obtained from RT-PCR of human T cell total RNA and subcloned into the mammalian expression vector pcDNA5/FRT/TO/TOPO (Invitrogen). The full-length hOrai1 and hOrai3 cDNAs were purchased from Origene and subcloned into the EcoRI and XhoI sites of pcDNA3 vector (Invitrogen). hOrai1 E106D mutant was created by exchanging the corresponding codons (GAG to GAT) using the QuikChange site-directed mutagenesis kit (Stratagene). The pcDNA5/HA-C-hSTIM1 clone (residues 235–685) was made by adding the HA tag to the corresponding cDNA by PCR and cloned into pcDNA5/FRT/TO/TOPO. For co-immunoprecipitation, N-terminal HA- or FLAG-tagged versions of hOrai1, hOrai2, and hOrai3 were made by introducing an in-frame EcoRI site after the first methionine of the coding sequence and subcloning the corresponding cDNA into a pCI (Promega)-derived vector (gift from Dr. F-A. Rassendren) between the EcoRI site following the tag sequence and either the BamHI or NotI or SalI site. For other experiments, N-terminal Myc-tagged versions of hOrai1, hOrai2, and hOrai3 were made by adding the Myc tag to the corresponding cDNA through PCR and cloned into pcDNA5/FRT/TO/TOPO. The Orai1–3 chimeras were made through two rounds PCR-based ligation (Roche Applied Science) and were cloned into pcDNA5/FRT/TO/TOPO. The resulting clones were confirmed by sequencing. Information on the primer design and conditions for cloning and PCR is available upon request.

RNAi in HEK293 Cells—For each of STIM1 and Orai1, a mixture of four siRNAs was purchased from Dharmacon. HEK293 cells were transfected by DNA plasmids and/or siRNAs using a Nucleofector (Amaxa) following the manufacturer's protocol.

RNA Isolation and RT-PCR—Total RNA was isolated using TRIzol reagent (Invitrogen) following the manufacturer's protocol. The methods for RT-PCR were the same as described before (14).

Immunocytochemistry—The methods for cell preparation were the same as described (15). Anti-Myc monoclonal antibodies (Santa Cruz Biotechnology) were used at a dilution of 1:50. Stained cells were viewed under a confocal laser scanning microscope LSM510 META (Zeiss).

Single-cell $[Ca^{2+}]_i$ Imaging—Ratiometric $[Ca^{2+}]_i$ imaging was performed as described (12), using the same solution composition. Transfected cells were identified by the co-expressed enhanced green fluorescent protein (GFP), using filters to avoid contamination of Fura-2 fluorescence by bleed through of GFP fluorescence (34). Data were analyzed with Metafluor software (Universal Imaging) and OriginPro 7.5 software (OriginLab) and are expressed as means ± S.E.

Patch Clamp Recording—CRAC current in the whole-cell mode was recorded as described previously (12, 35). The standard Cs^+-containing pipette solution consisted of (mM) the following: 130 cesium glutamate, 8 NaCl, 0.9 $CaCl_2$, 12 EGTA, and 10 HEPES. This solution was supplemented with 10 mM $MgCl_2$ to inhibit the endogenous Mg^{2+}-inhibited cation (MIC/TRPM7) channels (12). In some experiments, 6.5 or 8 mM $MgCl_2$ was used. The free Ca^{2+} concentration was ~100 nM as calculated by the Maxchelator program (available on line). Diffusion of EGTA, a strong Ca^{2+} buffer, into the cytosol results in gradual Ca^{2+} store emptying (9), and this method of "passive" store depletion was primarily used in this study. The standard extracellular solution contained (mM) the following: 150 sodium aspartate, 2 mM $CaCl_2$, 4.5 KCl, 10 Na-HEPES. In experiments with elevated Ca^{2+}, 4 mM $CaCl_2$ was added to this solution. For solutions containing 20 mM Ca^{2+} or 20 mM Mg^{2+}, divalent was added as the aspartate salt. In experiments with divalent-free solutions, 2 mM $CaCl_2$ was replaced with HEDTA, unless specified. For sodium replacement, 150 Na^+ aspartate was replaced with choline aspartate. All recording solutions used were buffered at pH 7.3. A glass coverslip plated with transfected HEK293 cells was mounted on the stage of a Zeiss IM35 microscope equipped with a HBO 50-watt arc lamp for detection of enhanced GFP fluorescence and patch clamp. Currents were recorded using an EPC-9 PC-driven patch clamp amplifier (HEKA Elektronik). Command voltage protocol generation and data acquisition were done using PULSE/PULSEFIT (HEKA Electronik). Data analysis was performed with Origin software. Patch pipettes were manufactured from borosilicate glass capillaries (Garner Glass) and had resistances in the range of 1–3 megohms. The ground silver-silver chloride electrode was connected to the bath through an agar bridge. All recordings were performed at room temperature.

Co-immunoprecipitation—Two days after transfection, 35-mm dishes plated HEK293 cells were washed twice with ice-cold PBS, lysed in 500 μl of RIPA lysis buffer (Upstate), supplemented with 1× Complete EDTA-free protease inhibitor mixture (Roche Applied Science), and passed five times through a 26-gauge needle. After 30 min of solubilization at 4 °C under agitation, lysates were centrifuged (16,000 × *g*, 10 min, 4 °C), and the supernatants were collected. Equal amounts of protein (750 μg) were diluted at 0.75 μg/μl in lysis buffer and mixed with either anti-HA-probe monoclonal antibody-conjugated agarose beads (1 μg per 100 μg total protein, Santa Cruz Biotechnology) or anti-FLAGM2 monoclonal antibody-conjugated agarose beads (40 μl of gel suspension per 750 μg of total protein, Sigma) overnight at 4 °C on a rotating wheel. Beads were washed three times (5 min at 4 °C) with 1 ml of lysis buffer. Proteins were eluted by incubation with 20 μl of 200 mM glycine, pH 2.2, neutralized with 4 μl of 1 M Tris-HCl, pH 8.5, and diluted in lithium dodecyl sulfate sample buffer (Invitrogen). Samples were resolved by SDS-PAGE and analyzed by standard Western blotting. Immunoblots were incubated with the primary antibodies indicated, including mouse anti-HA peroxidase-coupled (Roche Applied Science) 1:500 in PBS, 0.5% casein, 1 h at room temperature; mouse anti-FLAG M2 perox-

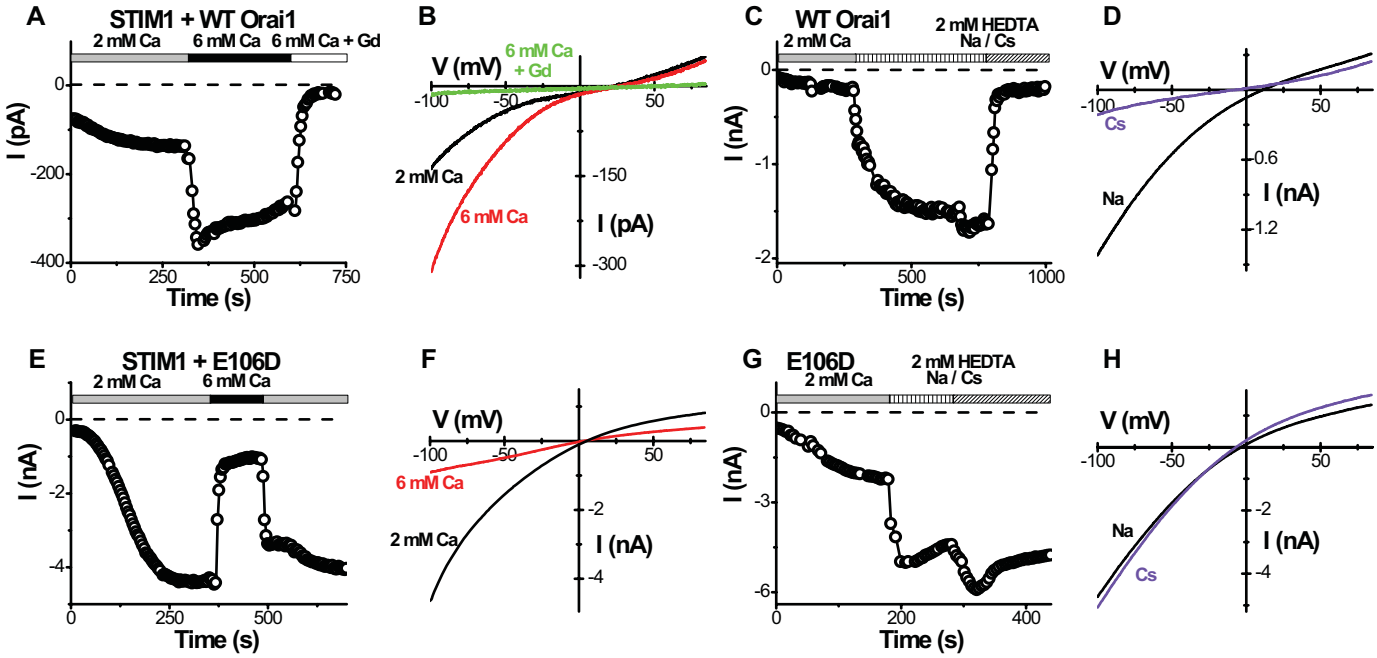

FIGURE 1. **Orai1 is the pore-forming subunit of the CRAC channel.** *A–D,* time course and *I-V* curves in representative cells overexpressing wild-type STIM1 and Orai1. *A,* inward CRAC-like current at −100 mV. Ca^{2+}-free internal solution. Solution exchanges are indicated. *B, I-V* curves for indicated external solutions. *C,* time course of current in divalent-free Na^+ or Cs^+ external solutions. Note absence of depotentiation for Na^+ current and much smaller current in Cs^+ external solution. *D, I-V* curves in divalent-free Na^+ or Cs^+ external solutions. *E–H,* corresponding time course and *I-V* curves in representative cells overexpressing wild-type STIM1 and Orai1 E106D mutant.

idase-coupled (Sigma) 1:2500 in PBS, 0.05% Tween 20, 1 h at room temperature; mouse anti-α-tubulin DM1A (Sigma) 1:2000 in PBS, 0.1% casein, 2 h at room temperature. Proteins were detected by developing with the ECL+ detection kit (GE Healthcare). Cells transfected only with one of the HA- or FLAG-tagged versions of hOrai1, hOrai2, and hOrai3 were used as controls.

RESULTS

Orai1 + STIM1 Overexpression Amplifies CRAC Current—HEK293 cells normally exhibit very little endogenous CRAC-like current (12, 13), even though the mRNAs of STIM1 and all three Orai genes are detectable by RT-PCR (supplemental Fig. S1*A*; see also Ref. 36). Consistent with previous reports (23–25), a large CRAC-like current was readily detected following co-transfection with Orai1 and STIM1, as illustrated by the time course of current development after break-in to achieve whole-cell recording in a representative cell (Fig. 1*A*). Typically, a component of CRAC-like current was detected immediately after achieving whole-cell recording in most cells; this pre-activated component constituted ~20–60% of the maximal current amplitude (see the pre-activated current at $t = 0$ in Fig. 1*A*). In cells transfected with Orai1 alone, no current was seen (data not shown). That most cells showed an activated current at break-in suggests that overexpressing STIM1 together with Orai1 may result in a "shortcut" activation of some CRAC channels, because of massive overexpression of STIM1 accompanied by an increase in localization near the plasma membrane, without prior Ca^{2+}-store emptying. The magnitude of the CRAC-like current increased as external Ca^{2+} was increased, as expected for a Ca^{2+}-selective channel, and displayed an inwardly rectifying current-voltage relation, typical for CRAC current (Fig. 1*B*). The small outward current seen at positive potentials represents a residual Mg^{2+}-inhibited cation (MIC) current of HEK cells (12). In the absence of external divalent cations, Na^+, but not Cs^+, was readily permeant in the expressed Orai1/CRAC channels (Fig. 1, *C* and *D*), as observed previously for native CRAC channels (6, 35, 37–39). However, the inward Na^+ current usually did not decline, a process termed "depotentiation" (39). Except for the lack of depotentiation, these properties are in accord with many previous studies of native CRAC current.

Altered Selectivity with Inward Rectification Induced by E106D Orai1 Mutation—We previously showed that a point mutation (E180D) in the conserved S1–S2 loop of *Drosophila* Orai transforms the ion selectivity properties of CRAC current from being Ca^{2+}-selective with inward rectification to being selective for monovalent cations and outwardly rectifying (18). This site is aligned with a glutamate residue at position 106 of human Orai1. Two studies using various systems for overexpression, one in SCID patient T cells with virally expressed Orai1 (wild-type Orai1 and Orai1 mutants) to complement the R91W Orai1 mutation and one in a HEK cell line stably overexpressing STIM1 with Orai1 transiently transfected, showed that the corresponding E106D mutation in Orai1 results in an altered ion selectivity while retaining an inwardly rectifying *I-V* characteristic (20–22). To resolve whether reported differences in *I-V* shape are because of the method of expression or to inherent differences between current induced by Orai and Orai1, we expressed the E106D mutant together with STIM1. The E106D-induced current was inwardly rectifying (Fig. 1, *E* and *F*), in accord with three previous studies on human Orai1 (20–22), but different from the corresponding *Drosophila* Orai

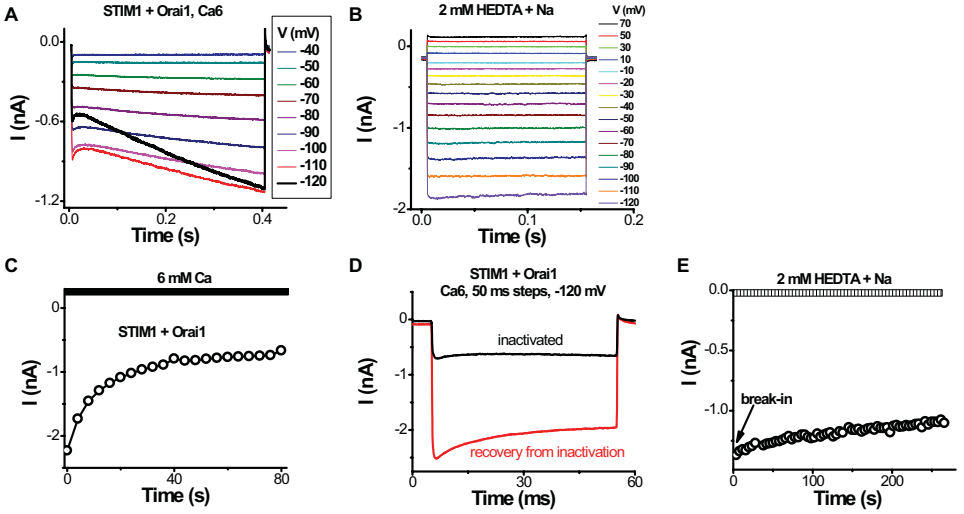

FIGURE 2. **Frequency-dependent and long pulse effects on CRAC-like current in HEK293 cells.** Recordings were done in cells overexpressing wild-type STIM1 and wild-type Orai1. *A,* selected current traces during voltage steps from −120 to 70 mV in 6 mM Ca^{2+} external solution. The trace at −120 mV was emphasized to show the unexpected time course. *B,* current during identical voltage steps in divalent-free Na^+ external solution. *C,* Ca^{2+}-induced inactivation assessed at −105 mV upon exposure to 6 mM Ca^{2+} external solution. Ramps were applied every 4 s. *D,* 50-ms pulses at −120 mV in 6 mM Ca^{2+} external solution. The *red trace* was recorded 1 min after the *black trace* was taken. The cell was at rest (held at 0 mV) between the two recordings. *E,* inward current development at −100 mV in the divalent-free Na^+ external solution from break-in. Note lack of depotentiation.

mutant (18). It reversed near 0 mV, much more negative than the WT channel (*cf.* Fig. 1*B*), indicating altered ion selectivity. In contrast to the WT channel, elevating external Ca^{2+} from 2 to 6 mM resulted in a substantial reduction of the inward current (Fig. 1, *E* and *F*), consistent with the block of current carried predominantly by monovalent cations. In contrast, the WT current magnitude was increased during the same maneuver as expected for a Ca^{2+}-selective channel (*cf.* Fig. 1*B*). The fact that E106D Orai1-induced current reversed at 0 mV in 2 mM Ca^{2+} and did not show any shift in reversal potential in 6 Ca^{2+} indicates that the E106D mutant Orai1 channel has lost its ability to conduct Ca^{2+} and instead primarily conducts monovalent cations. Cs^+, the only permeant internal cation, most probably carries the outward current seen at positive potentials. In agreement with this, the inward current in the absence of external divalent cations was carried equally well by Na^+ or Cs^+ (Fig. 1, *G* and *H*) (or by K^+; data not shown). In contrast, the WT Orai1-induced channel conducted Na^+ but not Cs^+ in the absence of external divalents (*cf.* Fig. 1, *C* and *D*). From these observations, the important conclusions are as follows. 1) The E106D mutation in Orai1 affects pore selectivity by abolishing Ca^{2+} permeation and selectivity among monovalent cations. 2) The inward rectification of CRAC channels is a fundamental property of the Orai1 pore and cannot be explained simply by an inability of Cs^+ to conduct in the outward direction at positive potentials.

Ca^{2+}-dependent Kinetics and Use Dependence—Rapid inactivation of inward currents was observed during hyperpolarizing voltage steps (Fig. 2*A*), as reported previously for the native current (6, 40). During hyperpolarizing steps, we noticed an additional time-dependent component of the current that was particularly pronounced at very negative potentials (Fig. 2*A*), consistent with a recent report (31). At −120 mV, the inward current increased significantly during the voltage step. Similar time dependence has been observed previously for native CRAC current in S2 cells, and it was suggested to be related to Ca^{2+}-dependent potentiation (33). Such time dependence was not seen for Orai1-induced monovalent currents recorded in the absence of external divalents (Fig. 2*B*). Applying voltage steps or ramps at high frequency resulted in a much slower current reduction over tens of seconds that was more evident in cells with higher levels of CRAC current (compare Fig. 1*A* and Fig. 2*C*). Current recovered from this slow inactivation after a period at the holding potential of 0 mV (Fig. 2*D*). Consistent with Ca^{2+} influx-inducing inactivation, we did not see current reduction when high frequency "loading" steps were applied in the absence of external divalents with Na^+ as the current-carrying ion (data not shown). Furthermore, the slow inactivation was not significant in the E106D mutant with reduced Ca^{2+} permeation even in highly expressing cells (Fig. 1*E*). Because the recordings were done in whole-cell mode with 12 mM EGTA in the pipette, we speculate that recovery from Ca^{2+}-dependent inactivation reflects chelation of Ca^{2+} by EGTA. We conclude that Orai1 and STIM1 overexpression is sufficient to reconstitute fast Ca^{2+}-dependent inactivation characteristic of endogenous CRAC channels (1, 40) and a slow Ca^{2+}-dependent inactivation similar to that reported previously (31). Depotentiation upon removal of external divalents was surprisingly limited in the overexpression system, even in intact cells, making it possible to record a large, pre-activated Na^+ current in divalent-free external solution immediately upon break-in (Fig. 2*E*).

Orai1 Activated by C Terminus of STIM1—The C-terminal portion of STIM1 (C-STIM1) expressed as a cytoplasmic protein was shown recently to interact with several transient receptor potential channels, canonical subfamily, and to induce activation of CRAC channels in Jurkat T cells (41). Consistent with this report, Jurkat cells transiently expressing the C-terminal STIM1 had higher resting Ca^{2+} levels and higher Ca^{2+} influx upon readmission of external Ca^{2+} following a period of exposure to external Ca^{2+}-free solution, in comparison with control cells expressing GFP as a marker of transfection or cells transfected with WT STIM1 (Fig. 3, *A*–*D*). The elevated Ca^{2+} levels were inhibited by the application of three different known CRAC blockers as follows: Gd^{3+} (1 μM), 2-APB (50 μM), and SKF96365 (20 μM) (data not shown). Thapsigargin (TG) was used to inhibit the sarco/endoplasmic reticulum Ca^{2+}-ATPase pump and deplete the stores. After depletion, the store-operated Ca^{2+} influx when C-STIM1 was expressed was somewhat lower than control, a result perhaps of feedback inhibition

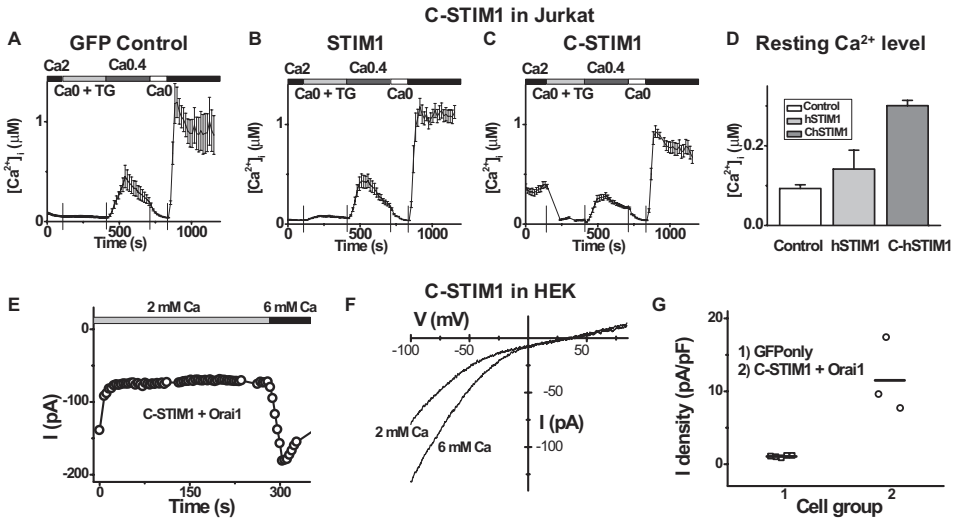

FIGURE 3. **C terminus of STIM1 is sufficient to pre-activate Orai1-induced Ca^{2+} influx and CRAC current.** *A–D*, C-STIM1 raises the resting Ca^{2+} level in Jurkat T cells by opening CRAC channels. Solution exchanges are indicated. *Vertical lines* indicate the time of solution exchange. Averaged $[Ca^{2+}]_i$ responses (±S.E.) in control (GFP only) Jurkat cells (*A*, $n = 9$ cells), Jurkat cells overexpressing full-length STIM1 (*B*, $n = 9$), and the C-terminal portion of STIM1 (C-STIM1) (*C*, $n = 21$). *D*, resting $[Ca^{2+}]_i$ in Jurkat cells (from *left to right*: $n = 11$, $n = 17$, and $n = 313$). *E*, time course of inward current at −100 mV in a representative HEK cell overexpressing C-STIM1 and wild-type Orai1. Ca^{2+}-free internal solution. Solution exchanges are indicated. *F*, *I-V* curves for indicated external solutions. *G*, current density determined in 2 mM external Ca^{2+} for 1) control HEK cells transfected with GFP only (*squares*), and 2) C-STIM1 + Orai1-overexpressing HEK cells (*circles*).

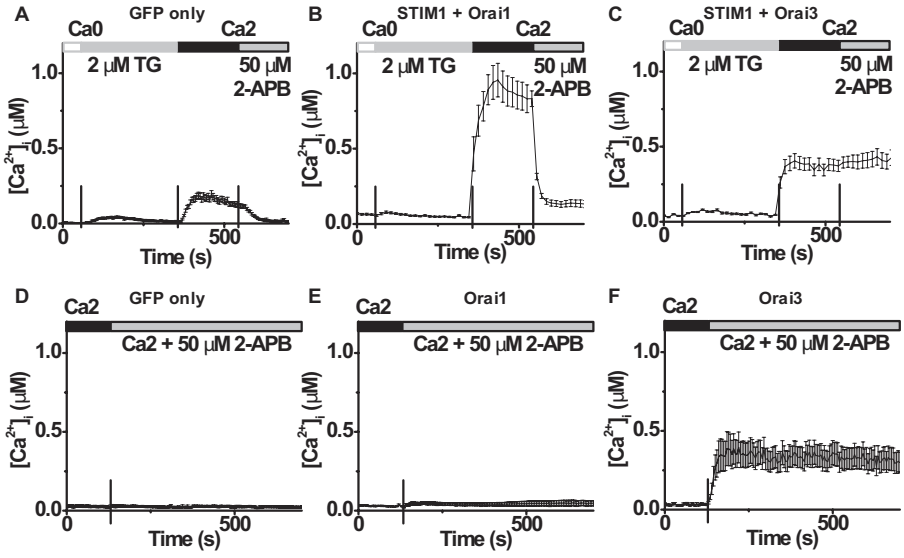

FIGURE 4. **Orai3, but not Orai1, can be activated by 50 μM 2-APB.** *A–C*, averaged $[Ca^{2+}]_i$ traces (±S.E.) before and following store depletion by addition of TG in cells transfected with GFP only (*A*, negative control, $n = 12$ cells), STIM1 + Orai1 (*B*, $n = 13$), and STIM1 + Orai3 (*C*, $n = 11$). *D–F*, averaged $[Ca^{2+}]_i$ traces (±S.E.) without store depletion in cells transfected with GFP only (*D*, $n = 8$ cells), Orai1 (*E*, $n = 6$), and Orai3 (*F*, $n = 8$). Solution exchanges are indicated.

because of prolonged elevation of cytosolic Ca^{2+}. These data indicate that native CRAC channels in Jurkat T cells are preactivated by expression of C-terminal STIM1. HEK cells also exhibited higher resting Ca^{2+} levels and higher Ca^{2+} influx upon readmission of external Ca^{2+} following co-expressing C-STIM1 and Orai1 (data not shown). To evaluate this further in the context of the amplified CRAC current paradigm, we confirmed a recent report (42) that a large CRAC current could be recorded immediately after break-in when C-STIM1 was co-expressed with Orai1 in HEK cells (Fig. 3, *E–G*). As expected the current was inwardly rectifying and could be augmented by supplementing the external Ca^{2+} concentration. The *I-V* shape was indistinguishable from that of fully developed CRAC current induced by full-length STIM1 plus Orai1 (*cf.* Fig. 1*B*).

Orai3 Ca^{2+} Influx Activated by 2-APB—To further compare the function of Orai homologs, human Orai1, Orai2, and Orai3 were transiently transfected with or without STIM1 into HEK cells. Increased expression levels were verified by RT-PCR (supplemental Fig. S1*B*). Interestingly, all three Orai members can form not only homo-multimers (supplemental Fig. S2*A*) but also hetero-multimers with any combination (supplemental Fig. S2*B*), which is in agreement with recent reports (21, 31, 36). However, under our transfection conditions we did not observe any significant increase of CRAC channel activity by expression of either Orai2 or Orai3 with STIM1 (supplemental Fig. S3), although Orai2, but not Orai3, inhibited Ca^{2+} influx and CRAC current induced by Orai1 (data not shown).

It has been reported recently that 2-APB can increase CRAC current following co-expression of Orai3 with STIM1 and inhibit CRAC current of Orai1 plus STIM1 (31). In intact HEK cells loaded with Fura-2, a small TG-evoked Ca^{2+} influx was completely suppressed by the application of 50 μM 2-APB (Fig. 4*A*) in control cells transfected with GFP only. In cells transfected with STIM1 plus Orai1, TG-evoked Ca^{2+} influx enhanced and was also strongly inhibited by 50 μM 2-APB (Fig. 4*B*). However, in cells overexpressing STIM1 with Orai3, addition of 2-APB produced no significant effect on $[Ca^{2+}]_i$ (Fig. 4*C*). Interestingly, in cells transfected with Orai3 alone (without STIM1), Ca^{2+} influx was also induced by the application of 50 μM 2-APB, even though the store was undisturbed while bathing cells in 2 mM Ca^{2+} Ringer's solution (Fig. 4*F*). In contrast, cells transfected with GFP only or Orai1 alone had no significant increase on resting Ca^{2+} upon addition of 2-APB (Fig. 4, *D* and *E*). Furthermore, knocking down endogenous STIM1 or Orai1 by siRNA in cells overexpressing Orai3 (supplemental Fig. S1*C*) did not significantly influence the 2-APB-evoked Ca^{2+} influx (supplemental Fig. S4). Thus, it is likely that 2-APB sensitizes or activates

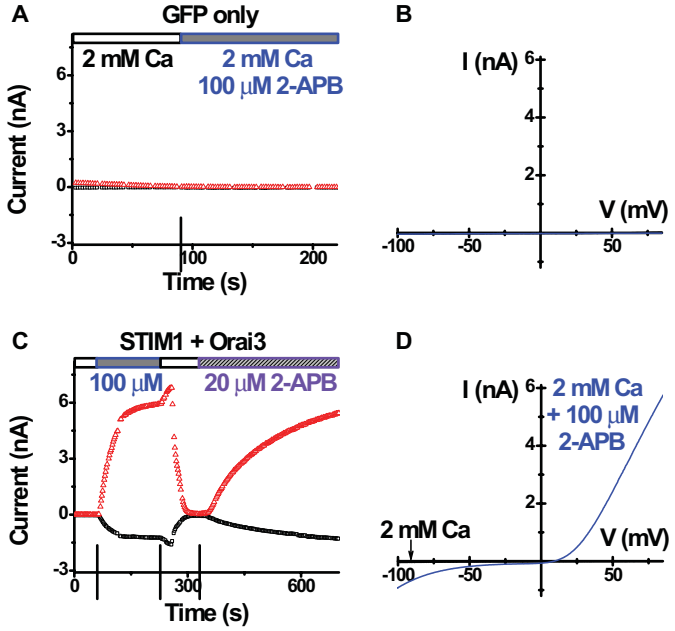

FIGURE 5. **2-APB-induced Orai3 current.** *A*, time course of both inward (−110 mV) and outward (+85 mV) current in a representative control HEK cell overexpressing GFP only. Ca^{2+}-free internal solution. *B*, *I–V* curves, before (*black trace*) and after (*blue trace*) application of 2-APB. Note there is little current under either condition. *C*, time course of current in a representative HEK cell overexpressing STIM1 and Orai3. *D*, *I–V* curves for indicated external solutions. Note the large current with both inward and outward components after 2-APB addition.

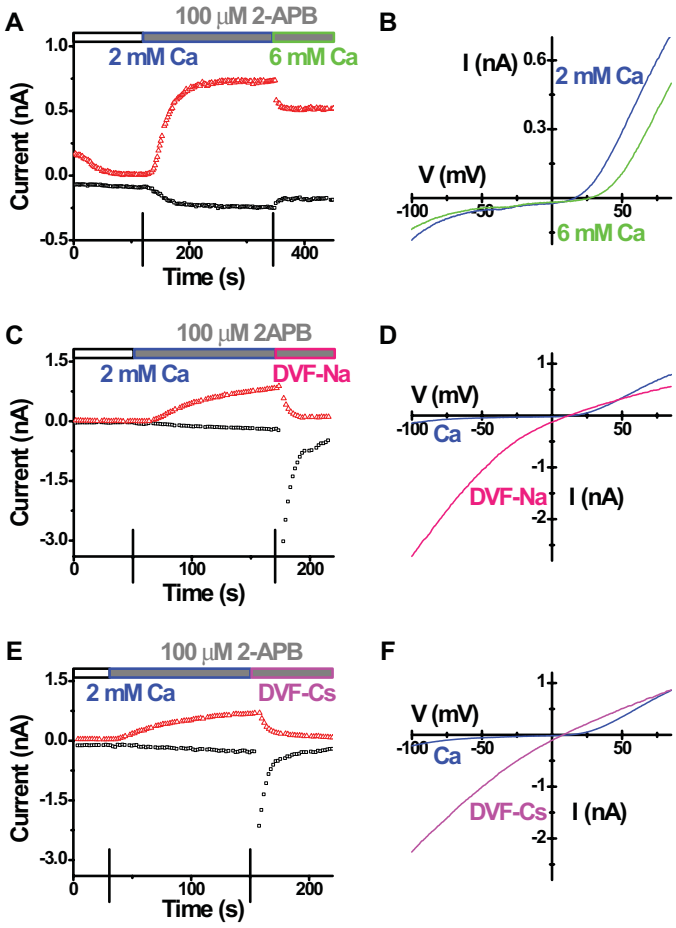

FIGURE 6. **Ion selectivity of 2-APB-induced Orai3 current.** Recordings were done in cells overexpressing wild-type STIM1 and wild-type Orai3. Corresponding time courses and *I-V* curves in representative cells tested for external Ca^{2+} change (*A* and *B*), Na^+ permeability (*C* and *D*), and Cs^+ permeability (*E* and *F*) after 2-APB addition. Solution exchanges are indicated.

channels formed by Orai3, bypassing the requirement for STIM1 or store depletion itself to open the Orai3 channels.

Orai3 Cation Current Evoked by 2-APB—We further examined the effect of 2-APB by whole-cell recording. In control cells transfected with GFP only (Fig. 5, *A* and *B*) or GFP + STIM1, there was no significant current development before or upon 2-APB addition. As expected, in cells transfected with STIM1 and Orai1, the reconstituted CRAC current was inhibited by the application of 50 or 100 μM 2-APB (data not shown), consistent with earlier reports on native and overexpressed CRAC currents (18, 31–33). On the other hand, as reported previously (31), application of 2-APB greatly enhanced inward current in cells overexpressing STIM1 and Orai3 (Fig. 5, *C* and *D*). However, we also observed an even larger outward current that was not reported previously (Fig. 5, *C* and *D*). Both inward and outward currents were diminished upon washout of external 2-APB and reappeared upon re-addition of 2-APB (Fig. 5*C*). The current amplitudes (both inward and outward) were similar when 50 or 100 μM 2-APB was applied; but 10 μM 2-APB had no apparent effect (data not shown).

We suspected that 2-APB may enlarge the channel pore by direct or indirect interaction with Orai3, allowing other cations to permeate. Two lines of evidence support this hypothesis. First, the current reversed near 20 mV, whereas typical CRAC current has a reversal potential larger than 50 mV under the same recording conditions. Second, 2-APB-induced current was slightly blocked by increasing external Ca^{2+} from 2 to 6 mM (Fig. 6, *A* and *B*). These results indicate that the 2-APB-induced current is not highly Ca^{2+}-selective. Furthermore, consistent with an increase in pore size, the 2-APB-induced current conducted either Na^+ or Cs^+ inwardly in the absence of external divalent cations (Fig. 6, *C–F*), whereas native CRAC current or Orai1 + STIM1-enhanced CRAC current are permeable only to Na^+ under the same recording conditions. Choline substitution of Na^+ in the external solution was used to examine the ionic basis of the inward component of the 2-APB-induced current. Replacing Na^+ with choline greatly decreased the size of inward current leaving a small remaining current (Fig. 7, *A* and *B*). Replacing both Na^+ and K^+ with choline in the external solution did not further change the current *I-V* shape (data not shown). These results indicate that the inward Orai3 current induced by 2-APB is carried predominantly by Na^+. When the external Ca^{2+} was increased from 2 to 20 mM, the inward current was not significantly changed (Fig. 7, *C* and *D*), suggesting that the enhanced mild blockage of Na^+ influx by elevated external Ca^{2+} concentration is balanced by the increased Ca^{2+} entry. Furthermore, replacement of 20 mM Ca^{2+} with 20 mM Mg^{2+} reduced inward currents (Fig. 7, *C* and *D*). These results indicate that both Na^+ and Ca^{2+} contribute to the 2-APB-induced inward current mediated by Orai3.

TM23 of Orai3 Mediates 2-APB Activation—A series of Orai1–Orai3 cDNA chimeras were prepared to identify the region of Orai3 that is responsible for 2-APB sensitization (sup-

plemental Fig. S5). The expression of all constructs was confirmed by Western blot (data not shown), and their surface localization was also verified by immunocytochemistry (supplemental Fig. S6). First, we screened all chimeras by single-cell Ca^{2+} imaging. Neither the N nor C terminus of Orai3, replacing the corresponding region of Orai1, was able to induce 2-APB sensitivity. In contrast, the transmembrane (TM) region of Orai3, expressed in the Orai1-TM-Orai3 chimera, fully mimicked the ability of full-length Orai3 to increase $[Ca^{2+}]_i$ after 2-APB stimulation (Fig. 8, *A–C*). We further dissected the Orai3 TM region into three overlapping elements, each containing two transmembrane segments and the loop in-between. A chimera containing the first two transmembrane segments of Orai3, Orai1-TM12-Orai3, had a small or negligible effect (Fig. 8*E*), and the last two transmembrane segments of Orai3 in the chimera Orai1-TM34-Orai3 had no response to 2-APB at all (Fig. 8*G*). However, the middle two transmembrane segments of Orai3, expressed as the Orai1-TM23-Orai3 chimera, appeared fully capable of generating 2-APB-evoked Ca^{2+} influx, comparable with Orai3 (Fig. 8*F*). Similarly, when co-expressed with STIM1, only the Orai1-TM-Orai3 chimera and the Orai1-TM23-Orai3 chimera mimicked full-length Orai3 (supplemental Fig. S7). The first and second loops between transmembrane segments were switched from Orai3 to Orai1 individually and were also tested. Although the Orai1-loop1-Orai3 chimera had no significant response to 2-APB as expected (Fig. 8*D*), the Orai1-loop2-Orai3 chimera exhibited a partial response to 2-APB, consisting of a transient elevation of $[Ca^{2+}]_i$ upon 2-APB addition (Fig. 8*H*). The two positive chimeras, Orai1-TM-Orai3 and Orai1-TM23-Orai3, that exhibited a strong enhancement of Ca^{2+} entry induced by 2-APB were then co-expressed with STIM1 and evaluated by patch clamp. 2-APB (100 μM) induced current in both chimeric channels (Fig. 9, *A* and *C*), with the same *I-V* shape as Orai3 (Fig. 9, *B* and *D*). In summary, these data suggest that the TM2, loop2, and TM3 of Orai3 are required for 2-APB, directly or indirectly, to open the Orai3 channel to admit cations nonselectively (supplemental Fig. S8).

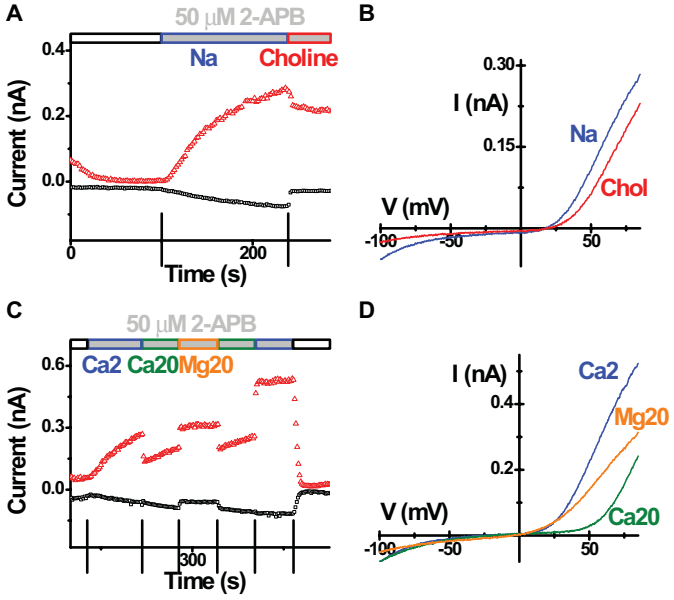

FIGURE 7. **2-APB-induced Orai3 current is carried by both Na^+ and Ca^{2+}.** Recordings were done in cells overexpressing wild-type STIM1 and wild-type Orai3. Corresponding time courses and *I-V* curves in representative cells tested for choline substitution (*A* and *B*) and Ca^{2+} replacement (*C* and *D*) in the presence of 50 μM external 2-APB. Solution exchanges are indicated.

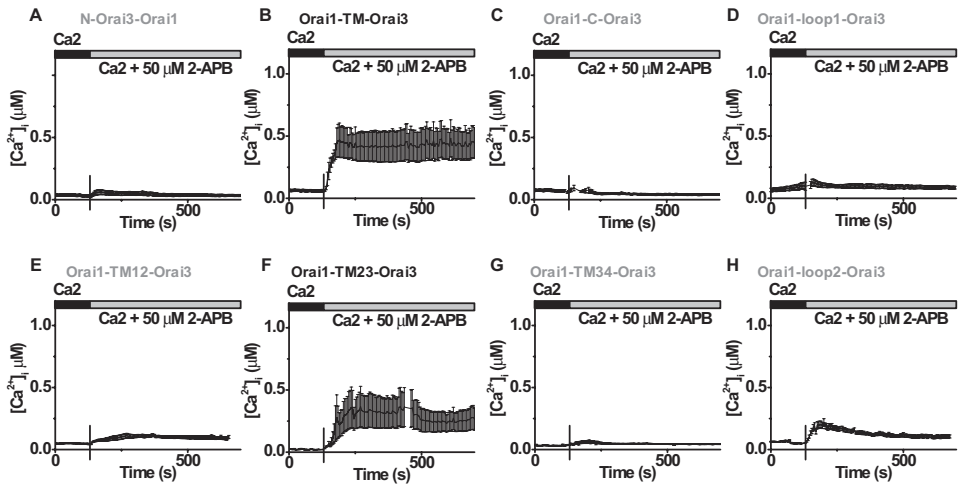

FIGURE 8. **TM23 of Orai3 is responsible for 2-APB sensitization/activation.** Averaged $[Ca^{2+}]_i$ traces (±S.E.) without Ca^{2+} store depletion in cells transfected with N-Orai3-Orai1 (*A*), Orai1-TM-Orai3 (*B*), Orai1-C-Orai3 (*C*), Orai1-loop1-Orai3 (*D*), Orai1-TM12-Orai3 (*E*), Orai1-TM23-Orai3 (*F*), Orai1-TM34-Orai3 (*G*), and Orai1-loop2-Orai3 (*H*). Solution exchanges are indicated.

2-APB-induced Ca^{2+} Influx and Current Require the Pore Loop of Orai3—To test the possibility that some unknown endogenous channel forms the pore that carries 2-APB-induced current, a pore mutant of Orai3 channels, E81A Orai3 with a mutation corresponding to E106A in Orai1 (see Fig. 1) in the first extracellular loop between transmembrane segments 1 and 2, was overexpressed and examined in Ca^{2+} imaging and whole-cell recording. The glutamate to alanine point mutation in the pore region had a strong dominant-negative effect on native SOCE. Comparing Fig. 10*A* to Fig. 4*A* illustrates that TG-induced Ca^{2+} entry was strongly suppressed in cells overexpressing both STIM1 and Orai3 E81A mutant. Interestingly, store-independent Ca^{2+} entry was not induced by 2-APB in cells overexpressing Orai3 E81A only (Fig. 10, *B* and *C*). This suggests that the critical glutamate in the first transmembrane loop of Orai3 mediates 2-APB evoked Ca^{2+} entry. This result was confirmed by patch clamp recording (Fig. 10*D*). In contrast to the large 2-APB current in cells overexpressing STIM1 plus wild-type Orai3, only a very small current developed in either direction in cells transfected with both STIM1 and Orai3 E81A mutant after the application of 100 μM 2-APB.

DISCUSSION

Ca^{2+} entry through store-operated channels following depletion of the ER Ca^{2+} store is a ubiquitous and essential homeostatic and cell signaling mechanism. The following

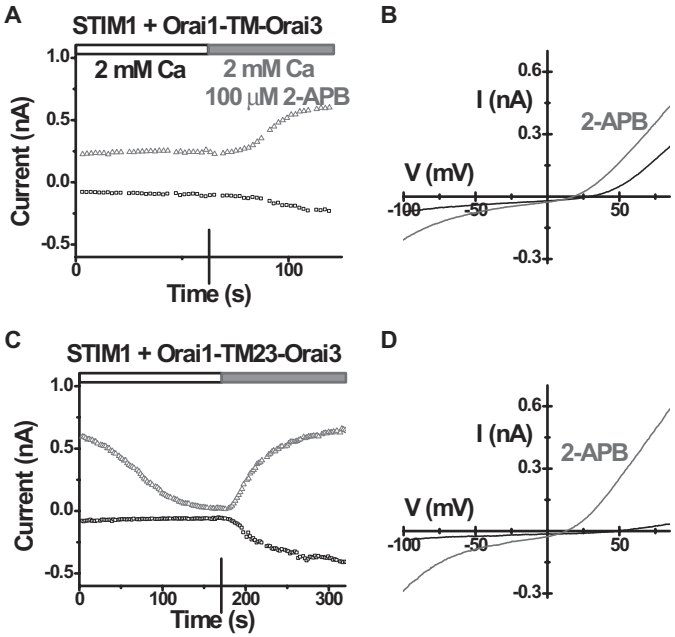

FIGURE 9. **2-APB-induced current from Orai1-Orai3 chimeras.** *A,* time course of both inward (−110 mV) and outward (+85 mV) current in a representative HEK cell overexpressing STIM1 and Orai1-TM-Orai3. Ca^{2+}-free internal solution. *B, I–V* curves before (*black*) and after (*grey*) 2-APB application. Note the *black trace* represents a relatively large endogenous MIC current. *C,* time course of current in a representative HEK cell overexpressing STIM1 and Orai1-TM23-Orai3. *D, I–V* curves for indicated external solutions.

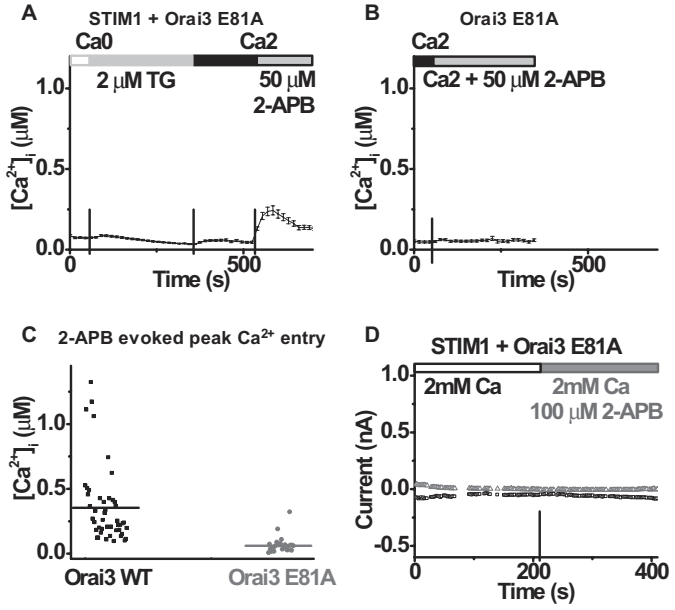

FIGURE 10. **Dominant-negative Orai3 mutant strongly suppresses the 2-APB effect.** *A,* averaged $[Ca^{2+}]_i$ traces (±S.E.) in cells transfected with STIM1 and Orai3 E81A. *B,* averaged $[Ca^{2+}]_i$ traces (±S.E.) in cells transfected with Orai3 E81A. *C,* peak 2-APB-induced Ca^{2+} influx values for cells overexpressing wild-type Orai3 (*bar 1*, $n = 46$ cells) and cells overexpressing Orai3 E81A mutant (*bar 2*, $n = 28$). *Horizontal lines* indicate the mean value in each group. $p < 0.00001$. *D,* time course of both inward (−110 mV) and outward (+85 mV) current in a representative HEK cell overexpressing STIM1 and Orai3 E81A. Solution exchanges are indicated.

three recent discoveries provide the basis for further investigation of molecular factors that are necessary for functional CRAC channel activation: the identification of Stim and Orai by RNAi screening; identification of their roles as the ER Ca^{2+} sensor and the pore-forming subunit of the CRAC channel, respectively; and the requirement for their co-expression to produce amplified CRAC current. In this study, human homologs of both molecules are manipulated in a heterologous expression system to target the specific domains and sites for channel gating and ion permeation properties. Inward rectification is retained in the pore mutant of Orai1 that alters ion selectivity. Our results confirm a recent report (42) that the C-terminal portion of STIM1 is sufficient to activate CRAC-like channel activity in Orai1. In addition, we show that Orai3, but not Orai1, can be activated by 2-APB, through a region including its 2nd and 3rd transmembrane segments and the loop in-between, to form a relatively nonselective cation pore. It is now apparent that CRAC channels can be opened either by STIM1 following store depletion, in a store-independent manner by EF-hand mutant STIM1, or by the C-terminal portion of STIM1, or, at least for Orai3, by 2-APB probably acting directly on the channel.

Activation by Store Depletion via STIM1—The sequence of events that link Ca^{2+} store depletion to CRAC channel activation is becoming clarified. The ER Ca^{2+} sensor function has been assigned to the EF hand motif located near the N terminus of STIM1 (11, 15). Following Ca^{2+} store depletion, STIM1 aggregates and migrates to the plasma membrane forming puncta at ER-plasma membrane junctions (11, 15–17, 19). STIM1 then induces redistribution of Orai1 into punctae that correspond to the sites of Ca^{2+} entry (16). We previously showed that Ca^{2+} store depletion strongly enhances interaction of the complete Stim protein with Orai, assessed by reciprocal co-immunoprecipitation (18). The mammalian homolog Orai1 was also shown to interact with STIM1 without prior store depletion, but effects of store depletion were not reported (21). More recently, a close molecular association has also been demonstrated by an increase in fluorescence resonance energy transfer between the C terminus of STIM1 and the C terminus of Orai1 following Ca^{2+} store depletion (42). Collectively, these results indicate that STIM1 (Stim) aggregation and migration to the plasma membrane following Ca^{2+} store depletion leads to a close molecular interaction with Orai1 (Orai), either directly or in a complex that corresponds temporally and spatially to the activation of CRAC channels.

Store-independent Activation of Orai1—Previous studies have shown that mutation of the EF-hand domain of STIM1 leads to constitutive activation of CRAC channel activity (11, 15). We demonstrate here that expression of the C-terminal fragment of STIM1 is sufficient to pre-activate overexpressed Orai1 channels by whole-cell current recording in HEK cells and native CRAC channels by single-cell Ca^{2+} imaging in Jurkat cells. These results confirm previous studies suggesting that the C-terminal portion of STIM1 is the effector domain that activates native CRAC current (41) and the CRAC channel pore formed by Orai1 (42). C-STIM1 may thus provide a useful tool for bypassing the requirement for store depletion in CRAC channel activation.

Store-independent Activation of Orai3 by 2-APB—It has been reported that 2-APB can activate several TRP channels, including TRPV1, TRPV2, and TRPV3 (27–30). Here we show that 2-APB can also activate Orai3 channels, confirming and

extending a previous report (31). The 2-APB-induced channel activity developed rapidly and without store depletion, perhaps by direct action on the Orai3 channel. Although not reported previously (31), the current induced by 2-APB likely results from a dilation of the Orai3 pore, converting the pore from being highly Ca^{2+} selective to one that conducts a mixture of monovalent and Ca^{2+} ions. The dynamic interaction between STIM1 and Orai1 is reported to be mediated by a putative coiled-coil region in the C terminus of Orai1 (42). Our chimera experiments support a key role of the transmembrane region of Orai3, rather than the C terminus, in conferring sensitivity to 2-APB. The transmembrane segments are important for Orai1 oligomerization (43). The large 2-APB-induced current was not seen with the Orai3 E81A mutant designed to be nonconducting in accord with the corresponding critical glutamate of Orai1; functional expression of Orai3 E81A was confirmed by its dominant-negative suppression of native SOCE in HEK cells. These results indicate that Orai3 itself carries the current induced by 2-APB. At this stage, it is not clear whether 2-APB sensitization of Orai3 channels is relevant to any endogenous CRAC behavior, but it may represent a previously undescribed mechanism to activate a nonselective cation conductance through Orai3 channels. Thus, 2-APB would be a very useful tool to examine the endogenous function of Orai3 in tissues with relatively high expression of Orai3 mRNA.

CRAC Channel Pore and Ion Selectivity—We sought to confirm that Orai1 controls ion permeation of the mammalian CRAC channel pore subunit, and to determine whether several biophysical properties of CRAC current are intrinsic to the pore. Consistent with previous reports (20–22), we found that the human Orai1 E106D point mutant significantly alters ion selectivity of the CRAC channel, indicating that Orai1 lines the selectivity filter of the CRAC channel. In external solution containing 2 or 6 mM Ca^{2+}, we observed an inwardly rectifying *I-V* relationship in wild-type and the E106D mutant, differing only in the extent of the outward current, because of Cs^+ in the pipette being impermeant in the native channel but able to carry significant current in the mutant. Increased permeability to Cs^+ in the E106D mutant also results in a shift of the reversal potential toward 0 mV, and in a greatly increased ability of Cs^+ to carry current upon divalent removal. Raising external Ca^{2+} blocks the inward current in the E106D mutant, instead of increasing the current as would be expected in a Ca^{2+}-selective channel. Generally, these results confirm that the E106D mutant may have a larger pore diameter than the wild type and conduct monovalent cations preferentially, with external Ca^{2+} block shaping the *I-V* relation, consistent with previous studies on Orai1 (20–22). However, the *I-V* shape of the E106D Orai1 pore mutant differs from that of the corresponding *Drosophila* Orai mutant (E180D) reported previously by our group (18). The difference in rectification of E180D Orai (outwardly rectifying) from E106D Orai1 (inwardly rectifying) implies that additional residues besides the critical glutamate must contribute to inward rectification of Orai1 when Glu-106 is mutated. The E106D mutant can conduct Cs^+ equally well as Na^+ in the absence of external divalents, and it still has an inwardly rectifying *I-V* characteristic with Cs^+ as the only permeant ion on both sides. This further demonstrates that inward rectification of CRAC current is because of its intrinsic pore properties rather than some blockage effect, in agreement with our previous findings for the native CRAC channel (35). Inward rectification cannot be simply explained as a consequence of a large gradient between extracellular and intracellular Ca^{2+}, because inward rectification persists in the E106D mutant when the current carrying species is equimolar Cs^+ on both sides of the membrane.

Interestingly, 2-APB addition generated a huge current through Orai3 channels with both inwardly and outwardly rectifying components. In contrast, Orai3 when activated by store depletion has been reported to have a similar *I-V* shape to Orai1 and native CRAC current (31). Similar to the current mediated by the Orai1 E106D mutant, we show that the 2-APB-induced Orai3 current conducts predominantly Na^+ (and to a lesser extent Ca^{2+}) inward and Cs^+ outward; additionally, the 2-APB-induced current can conduct both Na^+ and Cs^+ in the absence of divalent. This ability of 2-APB to activate the current in the absence of store depletion can be transferred to Orai1 (the current through which is completely blocked rather than promoted by 50 or 100 μM 2-APB) by replacing the TM23 of Orai1 with the corresponding region of Orai3, while leaving original loop1 region of Orai1, including the Glu-106 site that determines calcium selectivity, untouched. We are uncertain whether this represents the potential for an endogenous non-Ca^{2+}-selective SOC channel activity, but it certainly provides a linkage between CRAC channel gating and permeation. The 2-APB-induced current is abolished by a mutation of the corresponding glutamate (Glu-81 of Orai3) to alanine, indicating that the same store depletion-induced permeation pathway is used and suggesting that 2-APB opens the channel to a relatively dilated state that can admit monovalent cations, including even Cs^+.

Ca^{2+}-dependent Potentiation and Depotentiation of Monovalent CRAC Current—Several previous studies have shown that upon removal of external divalents, the CRAC current carried by Na^+ declines rapidly (6, 37, 38, 44). It is thought that in part this inactivation or depotentiation reflects the removal of potentiation because of previous exposure to external Ca^{2+}. Prakriya and Lewis (44) went further, postulating that depotentiation of monovalent CRAC current is a fundamental property of the CRAC channel, allowing it to be distinguished from other conductances. Our results suggest that Ca^{2+}-dependent potentiation and depotentiation may not be intrinsic to the channel pore, in contrast to ion selectivity and inward rectification. This is suggested by the large Na^+ current upon removal of external Ca^{2+} that did not decline significantly in the Orai1 + STIM1 overexpression system, and by the ability to record this Na^+ current immediately at break-in without pre-exposure to external Ca^{2+}. Thus, the Na^+ current can persist for many minutes with no apparent depotentiation. It was previously shown that monovalent CRAC current in RBL cells could develop with no apparent inactivation (37). Our own observations from different native systems are in accord with depotentiation being a cell-dependent rather than a channel-dependent phenomenon. For example, in human-activated T cell blasts, removal of Ca^{2+} results in an increased current showing almost no depotentia-

tion,[5] although the Na^+ current usually declines in tens of seconds in Jurkat T cells. These observations suggest that monovalent current inactivation may not be explained by the channel alone but rather is descriptive of the cellular membrane (components) where the channel resides, or the relative levels of STIM1, or Orai1 expression in different cells (*cf.* Ref. 45). Depotentiation of native monovalent CRAC current seen in S2 cells is retained for the amplified CRAC current when Stim and Orai are overexpressed in these cells (18), reinforcing the suggestion that the cell type may determine this aspect of CRAC channel gating.

Acknowledgments—We thank Lu Forrest for assistance in cell culture and Prof. George Chandy for use of molecular reagents in his laboratory.

REFERENCES

1. Parekh, A. B., and Putney, J. W., Jr. (2005) *Physiol. Rev.* **85,** 757–810
2. Cahalan, M. D., Zhang, S. L., Yeromin, A. V., Ohlsen, K., Roos, J., and Stauderman, K. A. (2007) *Cell Calcium* **42,** 133–144
3. Feske, S. (2007) *Nat. Rev. Immunol.* **7,** 690–702
4. Lewis, R. S. (2007) *Nature* **446,** 284–287
5. Lioudyno, M. I., Kozak, J. A., Penna, A., Safrina, O., Zhang, S. L., Sen, D., Roos, J., Stauderman, K. A., and Cahalan, M. D. (2008) *Proc. Natl. Acad. Sci. U. S. A.* **105,** 2011–2016
6. Hoth, M., and Penner, R. (1993) *J. Physiol.* (*Lond.*) **465,** 359–386
7. Hoth, M., and Penner, R. (1992) *Nature* **355,** 353–356
8. Lewis, R. S., and Cahalan, M. D. (1989) *Cell Regul.* **1,** 99–112
9. Zweifach, A., and Lewis, R. S. (1993) *Proc. Natl. Acad. Sci. U. S. A.* **90,** 6295–6299
10. Feske, S., Gwack, Y., Prakriya, M., Srikanth, S., Puppel, S. H., Tanasa, B., Hogan, P. G., Lewis, R. S., Daly, M., and Rao, A. (2006) *Nature* **441,** 179–185
11. Liou, J., Kim, M. L., Heo, W. D., Jones, J. T., Myers, J. W., Ferrell, J. E., Jr., and Meyer, T. (2005) *Curr. Biol.* **15,** 1235–1241
12. Roos, J., DiGregorio, P. J., Yeromin, A. V., Ohlsen, K., Lioudyno, M., Zhang, S., Safrina, O., Kozak, J. A., Wagner, S. L., Cahalan, M. D., Velicelebi, G., and Stauderman, K. A. (2005) *J. Cell Biol.* **169,** 435–445
13. Vig, M., Peinelt, C., Beck, A., Koomoa, D. L., Rabah, D., Koblan-Huberson, M., Kraft, S., Turner, H., Fleig, A., Penner, R., and Kinet, J. P. (2006) *Science* **312,** 1220–1223
14. Zhang, S. L., Yeromin, A. V., Zhang, X. H., Yu, Y., Safrina, O., Penna, A., Roos, J., Stauderman, K. A., and Cahalan, M. D. (2006) *Proc. Natl. Acad. Sci. U. S. A.* **103,** 9357–9362
15. Zhang, S. L., Yu, Y., Roos, J., Kozak, J. A., Deerinck, T. J., Ellisman, M. H., Stauderman, K. A., and Cahalan, M. D. (2005) *Nature* **437,** 902–905
16. Luik, R. M., Wu, M. M., Buchanan, J., and Lewis, R. S. (2006) *J. Cell Biol.* **174,** 815–825
17. Wu, M. M., Buchanan, J., Luik, R. M., and Lewis, R. S. (2006) *J. Cell Biol.* **174,** 803–813
18. Yeromin, A. V., Zhang, S. L., Jiang, W., Yu, Y., Safrina, O., and Cahalan, M. D. (2006) *Nature* **443,** 226–229
19. Liou, J., Fivaz, M., Inoue, T., and Meyer, T. (2007) *Proc. Natl. Acad. Sci. U. S. A.* **104,** 9301–9306
20. Prakriya, M., Feske, S., Gwack, Y., Srikanth, S., Rao, A., and Hogan, P. G. (2006) *Nature* **443,** 230–233
21. Vig, M., Beck, A., Billingsley, J. M., Lis, A., Parvez, S., Peinelt, C., Koomoa, D. L., Soboloff, J., Gill, D. L., Fleig, A., Kinet, J. P., and Penner, R. (2006) *Curr. Biol.* **16,** 2073–2079
22. Yamashita, M., Navarro-Borelly, L., McNally, B. A., and Prakriya, M. (2007) *J. Gen. Physiol.* **130,** 525–540
23. Mercer, J. C., Dehaven, W. I., Smyth, J. T., Wedel, B., Boyles, R. R., Bird, G. S., and Putney, J. W., Jr. (2006) *J. Biol. Chem.* **281,** 24979–24990
24. Peinelt, C., Vig, M., Koomoa, D. L., Beck, A., Nadler, M. J., Koblan-Huberson, M., Lis, A., Fleig, A., Penner, R., and Kinet, J. P. (2006) *Nat. Cell Biol.* **8,** 771–773
25. Soboloff, J., Spassova, M. A., Tang, X. D., Hewavitharana, T., Xu, W., and Gill, D. L. (2006) *J. Biol. Chem.* **281,** 20661–20665
26. Maruyama, T., Kanaji, T., Nakade, S., Kanno, T., and Mikoshiba, K. (1997) *J. Biochem.* (*Tokyo*) **122,** 498–505
27. Juvin, V., Penna, A., Chemin, J., Lin, Y. L., and Rassendren, F. A. (2007) *Mol. Pharmacol.* **72,** 1258–1268
28. Neeper, M. P., Liu, Y., Hutchinson, T. L., Wang, Y., Flores, C. M., and Qin, N. (2007) *J. Biol. Chem.* **282,** 15894–15902
29. Chung, M. K., Lee, H., Mizuno, A., Suzuki, M., and Caterina, M. J. (2004) *J. Neurosci.* **24,** 5177–5182
30. Hu, H. Z., Gu, Q., Wang, C., Colton, C. K., Tang, J., Kinoshita-Kawada, M., Lee, L. Y., Wood, J. D., and Zhu, M. X. (2004) *J. Biol. Chem.* **279,** 35741–35748
31. Lis, A., Peinelt, C., Beck, A., Parvez, S., Monteilh-Zoller, M., Fleig, A., and Penner, R. (2007) *Curr. Biol.* **17,** 794–800
32. Prakriya, M., and Lewis, R. S. (2001) *J. Physiol.* (*Lond.*) **536,** 3–19
33. Yeromin, A. V., Roos, J., Stauderman, K. A., and Cahalan, M. D. (2004) *J. Gen. Physiol.* **123,** 167–182
34. Fanger, C. M., Rauer, H., Neben, A. L., Miller, M. J., Wulff, H., Rosa, J. C., Ganellin, C. R., Chandy, K. G., and Cahalan, M. D. (2001) *J. Biol. Chem.* **276,** 12249–12256
35. Kozak, J. A., Kerschbaum, H. H., and Cahalan, M. D. (2002) *J. Gen. Physiol.* **120,** 221–235
36. Gwack, Y., Srikanth, S., Feske, S., Cruz-Guilloty, F., Oh-hora, M., Neems, D. S., Hogan, P. G., and Rao, A. (2007) *J. Biol. Chem.* **282,** 16232–16243
37. Bakowski, D., and Parekh, A. B. (2002) *Pfluegers Arch.* **443,** 892–902
38. Lepple-Wienhues, A., and Cahalan, M. D. (1996) *Biophys. J.* **71,** 787–794
39. Zweifach, A., and Lewis, R. S. (1996) *J. Gen. Physiol.* **107,** 597–610
40. Zweifach, A., and Lewis, R. S. (1995) *J. Gen. Physiol.* **105,** 209–226
41. Huang, G. N., Zeng, W., Kim, J. Y., Yuan, J. P., Han, L., Muallem, S., and Worley, P. F. (2006) *Nat. Cell Biol.* **8,** 1003–1010
42. Muik, M., Frischauf, I., Derler, I., Fahrner, M., Bergsmann, J., Eder, P., Schindl, R., Hesch, C., Polzinger, B., Fritsch, R., Kahr, H., Madl, J., Gruber, H., Groschner, K., and Romanin, C. (2008) *J. Biol. Chem.* **283,** 8014–8022
43. Li, Z., Lu, J., Xu, P., Xie, X., Chen, L., and Xu, T. (2007) *J. Biol. Chem.* **282,** 29448–29456
44. Prakriya, M., and Lewis, R. S. (2002) *J. Gen. Physiol.* **119,** 487–507
45. DeHaven, W. I., Smyth, J. T., Boyles, R. R., and Putney, J. W., Jr. (2007) *J. Biol. Chem.* **282,** 17548–17556

[5] J. A. Kozak, unpublished data.